



Laser ablation in water for silver and gold nanoparticle synthesis and their application for improvement of TEA CO₂ LIBS setup performance

Miloš Momčilović¹ · Jelena Petrović¹ · Milica Nemoda¹ · Jovan Ciganović¹ · Nikša Krstulović² · Miloš Ognjanović¹ · Sanja Živković¹

Received: 13 January 2023 / Accepted: 16 March 2023 / Published online: 31 March 2023
© The Author(s), under exclusive licence to Springer-Verlag GmbH Germany, part of Springer Nature 2023

Abstract

Pulsed laser ablation in liquids (PLAL) is an approach for the direct synthesis of nanoparticles from the bulk material. In the present work, silver and gold nanoparticles (NPs) were synthesized using the PLAL technique, and obtained water colloid suspensions were characterized by TEM–EDX, ICP–OES, UV–VIS, and DLS methods. On the other hand, Laser-Induced Breakdown Spectroscopy (LIBS) is a well-recognized and versatile analytical technique for the element analysis of solid samples. However, obtaining improved spectral intensity and detection sensitivity are still great challenging tasks, especially for an alternative and cost-effective LIBS setup based on TEA CO₂ laser. Considering these demands, this work aimed to investigate a promising approach to signal enhancement based on the deposition of noble NPs on the plastic sample. The effect of NPS on the enhancement of the LIBS signal has been investigated. LIBS experiments were carried out in air at atmospheric pressure and obtained spectra with a high signal-to-background (SBR) ratio. This study shows that signal enhancement can be achieved followed by the lower limits of detection by increasing the ablation amount rate.

1 Introduction

Plastic has become an integral part of human daily life and global plastics production and consumption raise from year to year. In 2019 worldwide production reached an all-time high record of about 370 million tons. Many additives and catalysts, that are added to plastic to give it better physico-chemical characteristics, are based on compounds of heavy metals. Insoluble inorganic compounds, partially soluble organic compounds, or salts may be used as metal-based additives [1]. For example, chromium (VI) trioxide (CrO₃) and lead oxide (PbO), are added to all plastics for pigmentation and to improve fastness, and heat stability [2]. At the same time, these elements become widespread in the environment and their impact as a contaminant has caused

significant attention in past decades. Very small quantities of Cr and Pb are toxic and might be lethal for the living world, while at very low concentrations and acute or chronic poisonings may occur following exposure through water, air, and food [3, 4]. Therefore, the degradation of plastic caused the diffusion of heavy metals from a matrix and represents a potential environmental problem. From an environmental perspective, the quality control of plastic products, with a special focus on the fast monitoring of heavy metals, raises more attention.

As an analytical “star in raising” with many obvious advantages, LIBS attaches more and more interest and importance to plastic investigations, with the capacity for simultaneous qualitative and quantitative analysis [5]. Generally, LIBS is an extremely versatile method that combines the capability of providing fast multi-elemental analysis with no or minimal sample pre-treatment, the potential for in-laboratory, in situ, and remote analysis, micro-destructiveness, the ability to provide isotopic ratio information and to perform multi-layered, depth profiling and qualitative or quantitative imaging measurements [6, 7].

However, despite all these advantages, compared to other standard and well-established spectrochemical methods for trace metal analysis such as Inductively Coupled Plasma

✉ Sanja Živković
sanjaz@vinca.rs

¹ VINCA Institute of Nuclear Sciences—National Institute of the Republic of Serbia, University of Belgrade, P.O. Box 522, 11351 Belgrade, Serbia

² Institute of Physics, Bijenička Cesta 46, 10000 Zagreb, Croatia

Optical Emission Spectrometry (ICP OES) or Atomic Absorption Spectroscopy (AAS), LIBS show relatively high Limits of Detection (LODs). Several different approaches have been investigated to overcome this deficiency. De Giacomo et al. introduced a promising method to improve LIBS sensitivity named Nanoparticle Enhanced Laser Induced Breakdown Spectroscopy (NELIBS) by using a micro-drop of a solution containing nanoparticles (NPs) deposited on the sample surface in an area covering the focused laser spot. Nanoparticles bring enhancement due to the lower thermal conductivity of small-sized objects under laser irradiation decreases the ablation threshold and laser-induced plasma absorbs energy from a larger temporal portion of the pulse. Consequently, the plasma plume resulting in this way will be at a higher temperature and has a longer lifetime, and the intensity of the emitted spectral lines will be stronger and has a much better signal-to-noise ratio which improves significantly the technique sensitivity [8]. The underlying mechanisms responsible for NELIBS are described in detail in a study by Dell'Aglio et al. [9].

In recent years, the NELIBS approach has been studied from various aspects by different research groups. Abdelhamid et al. studied the significance of nanostructure shapes in NELIBS and have shown that LIBS signal's achieved enhancement was the highest when using silver nanowires [10]. Composite Ag–Cu and Ni–C nanoparticles synthesized by laser ablation and spark discharge in liquid, respectively, have been used for NELIBS applications and the intensity growth was higher for Ag–Cu nanoparticles [11]. Also, Palásti et al. have shown that NELIBS signal enhancement approach can be used successfully in the quantitative analysis of liquid samples [12]. In a study by Salajkova et al. it was shown that the optimal NPs concentration is extremely important for a correct setup of the NELIBS experiment [13]. An alternative approach of NELIBS based on the direct mixing of gold nanoparticles (AuNPs) and metal chelates increased the contact area, adhesion force, and uniformity between analytes and AuNPs and significantly improve the NELIBS method [14]. Most recent study by Dell'Aglio et al. investigated systematically NELIBS performance using AuNPs of different shapes by optimizing the sample preparation procedure. They have shown that when the optimal concentration for each specific size and shape is selected, the maximum enhancement does not depend on the type of NP used [15]. On the other hand, the recent results obtained by Kiris et al. [16] that the presence of NPs significantly influences the analytical properties of plasma induced by Nd:YAG laser, however, doesn't significantly affect the analytical performance of LIBS based on TEA CO₂ laser.

Physical methodologies for the production of NPs used in NELIBS are strongly suggested because the colloidal solution should not have any unwanted residual byproducts and impurities that can interfere with the measured analyte

[9]. In the present article Ag and Au NP are synthesized by pulsed laser ablation in liquid (PLAL) as described in the experimental section. PLAL is a versatile and effective physical method of synthesis and appeared to be competitive with chemical techniques. First of all, it is an easy-to-handle and cost-effective method for the room-temperature synthesis of ultrapure nanomaterials [17]. PLAL is not limited by a choice of metal material because any metal can be ablated while synthesis can be done in a variety of liquids. PLAL is also recognized as an environmentally friendly technique because no chemicals are required for synthesis processes making this method impurities—and byproducts-free [18]. Generally, 'clean' PLAL nanoparticles' surfaces are much more active in their interaction with surrounding material and therefore are favorable for advanced ultra-sensitive techniques such as surface-enhanced Raman spectroscopy [19] or for applications in catalysis [20]. An additional advantage of PLAL over chemical methods is the stability of the colloidal solutions. Namely, the presence of chemicals may reduce the surface charge of the nanoparticles and thus electrostatic repulsion causing poor stability due to the formation of agglomerations and precipitation.

Our numerous previous papers demonstrated that an original and much more low-cost LIBS setup based on TEA CO₂ laser could be successfully applied for various applications and that it is fully comparable in analytical capabilities to much more expensive ones [21–26]. Bearing in mind, that the most important characteristic of our laser is its temporal profile of pulse which is composed of a peak (duration of about 100 ns) followed by a long-lasting tail (duration of about 2 microseconds) [21] and because of that TEA CO₂ laser has a favorable condition for obtaining long-lasting highly excited plasma. The plasma is formed during the interaction of the initial portion of the laser pulse with the target while the tail reheats the plasma, elongates its lifetime, and increases the LIBS signal. The effect is similar to a dual pulse excitation that was shown to provide enhancement of plasma emission [27]. It is expected that NELIBS additionally improves excitation conditions in plasma and finally increases the LIBS signal.

The aim of the present research was to assess the feasibility of additional improving the analytical performances of this unique setup, without raising the cost of the equipment, since NELIBS technique is becoming a very promising method in the LIBS community. Moreover, the motivation for this work was the detection of heavy metals in plastics, because, to the best of our knowledge, no report has been published on the use of the CO₂ laser for this purpose. Additionally, we fabricated solutions of Ag and Au NPs and investigated their NELIBS analytical performance.

2 Materials and methods

2.1 Nanoparticle synthesis

PLAL synthesis of noble nanoparticles was performed by using two independent Nd:YAG setups.

A pure gold target (GoodFellow, UK, purity > 99.9%) was immersed in 25 ml of Milli-Q water and placed about 2.5 cm under the water surface. The sample surface of approximately 1 cm² in size was continually scanned to achieve a homogenous ablation by a pulsed laser beam. The total number of pulses for irradiation was 2000 using the Nd:YAG laser (300 mJ output energy, 5 Hz repetition rate, 5 ns pulse duration, wavelength of 1064 nm, Quantel, Brilliant). The laser beam was focused by a 10 cm lens to enhance the ablation yielding the laser fluence of 25 J/cm². A detailed experimental setup is shown in [28].

A pure silver target (Alfa Aesar, DE, purity 99.9985%) was covered with 6 ml of Milli-Q water. The treated sample surface was approximately the same as for the gold target and it was continually scanned by a pulsed laser beam of Nd:YAG laser (20 mJ, 10 Hz, 150 ps pulse duration, wavelength of 1064 nm, EKSPILA SL 212/SH/FH) for 25 min. The laser beam was focused by a 15.3 cm lens to enhance the ablation yielding the laser fluence of 28 J/cm².

Characterization of formed nanocolloids was performed with the measurement of the SPR band using a UV–VIS spectrophotometer (LLG-uniSPEC 4 UV/VIS-Spectrophotometer). The averaged hydrodynamic diameters (d_H) were estimated by dynamic light scattering (DLS), measured on a Zetasizer Nano ZS90 apparatus (Malvern, UK) with a 4 mW 633 nm He–Ne laser source. The measurements were performed in disposable polystyrene cuvettes (DTS0012) at ambient temperature (25 ± 0.1 °C). Also, NP concentration as an important parameter for signal enhancement was determined by ICP-OES spectrometer (Thermo Scientific iCap 7400 duo). The calibration standard solutions of both elements were prepared from a single element stock standards J.T. Baker (1000 µg/ml) by diluting to different volumes of distilled deionized water with 1% high-purity HNO₃ (w/w). The data acquisition and processing were performed by using The Thermo Scientific Qtegra Intelligent Scientific Data Solution (ISDS) software. The obtained results are presented in the form of the average values of three measurements.

For morphology study, NPs were investigated by transmission electron microscopy (TEM) at 200 kV acceleration voltage. The images were recorded on a Talos F200X electron microscope from FEI Company, equipped with a CCD camera with a resolution of 4096 × 4096 pixels using the User Interface software package. An energy-dispersive X-ray spectroscopy (EDX) system attached to the TEM

operating in the scanning transmission (STEM) mode was used for chemical analysis and element color mapping. High-angle annular dark-field (HAADF) images were captured in nanoprobe-TEM mode with probes of below 1 nm size and a camera length of ~ 200 mm. The samples for TEM examination were prepared by a standard procedure where a drop of the water solution was placed on a carbon-coated copper grid, which was allowed to dry in the air.

2.2 LIBS setup and NELIBS experiments on the polypropylene sample

The TEA CO₂ laser developed at VINCA Institute was used as an excitation source for plasma generation. The laser energy was measured in front of the ZnSe lens with Joulemeter ED-200 through a Tektronix TDS 1002 digital oscilloscope. Applied laser energy was 160 mJ with a repetition rate of 1 Hz and the shot-to-shot fluctuation of its energy was about 5%. The laser was run in a multimode regime. The angle of incidence of the laser beam with respect to the target surface was 90°. The optical emission from the plasma was viewed in the direction parallel to the sample surface. Time-integrated space-resolved laser-induced plasma spectroscopy (TISR LIPS) method was applied. This method provides enhance of signal background ratio by observing further-out regions of plasma where the plasma background continuum emission is largely reduced. The plasma emission was projected by an achromatic lens on the entrance slit of the monochromator Carl-Zeiss PGS2 (entrance slit width 30 µm, height 1 mm, magnification 1:1). The monochromator was equipped with a diffraction grating with 600 lines/mm (dispersion around 0.7 nm/mm, depending on the wavelength, blaze at 330 nm in the first order). The position-selective spectra were monitored by CCD camera Apogee Alta F1007, consisting of 1024 × 122 pixels, 12 × 12 µm each, and a total active area of 12.3 × 1.46 mm. A Mercury lamp was used for spectral calibration.

A sample of polypropylene plastic (PP) used for medical waste disposal container production was selected for these experiments. Before LIBS experiments, the concentration of Pb and Cd in a plastic sample was determined by ICP-OES. A sample of PP was digested using a TANK microwave digestion system (SINEO, CN) and ACS-grade nitric acid and hydrogen peroxide. For calibration 1000 mg/L Multi-element ICP Standard solution (Chem-Lab, Belgium) was used. The sample was prepared in duplicate and ICP-OES measurements were performed in triplicate.

Nanoparticles of silver and gold were applied in a thin layer on the surface of the plastic sample with a micropipette and left to dry in an oven. The shutter of the non-gated CCD detector was opened for 6 s and in this way, two consecutive spectra were acquired without time resolution. The optimization of the spectral emission was achieved by applying

the TISR-LIBS method, where the spectrum acquisition was performed in triplicate. In addition, the obtained spectra represent the average values of the emission signal measured from nine different parts of the sample surface.

2.3 Profilometric measurement

The effect of deposited nanoparticles on the ablation rate was evaluated using a non-contact Zygo 3 NewView 7100 Optical Surface Profiler which is based on the interference of the light beam reflected from the reference surface and the beam reflected from the examined surface. The main advantage of this method for surface characterization is that it is non-destructive and maintains surface characteristics. The surfaces of samples with or without nanoparticles, before and after irradiation with TEA CO₂ laser radiation, were analyzed. Data acquisition and analysis are performed using ZYGO MetroPro.

3 Results

3.1 Nanoparticle characterization

Confirmation of noble metal nanoparticle formation and plasmonic resonance can be found by analyzing the absorbance data of UV–Vis spectroscopy. In Fig. 1a, the UV–Vis spectra showed characteristic peaks at 428 nm and 525 nm, which correlate to the surface plasmon absorbance of Ag and Au nanoparticles, respectively. The hydrodynamic diameters of noble nanoparticles solution at pH 6, were determined by the DLS method and the obtained d_H value was 110 nm for AuNPs, while in the case of AgNPs, agglomeration occurs and two groups were detected, a smaller one at 25 nm and

larger one at 200 nm, Fig. 1b. Total concentrations measured by ICP-OES were 8.7 ± 0.1 and 49.2 ± 0.1 $\mu\text{g/ml}$ for Au and AgNPs, respectively.

Furthermore, the size and morphology of these nanoparticles were also estimated by TEM images and EDX analysis. Typical images are shown in Fig. 2. The observed nanoparticles are mainly spherical and pseudospherical and partially agglomerated. The size distributions of Au and Ag NPs were determined by manual measurement of about 100 particles using the public domain software ImageJ [27]. After statistical analysis, it was found that the particle size of AgNPs was $d_{TEM} = 29.7 \pm 10.4$ nm, while the size of AuNPs was $d_{TEM} = 46 \pm 26$ nm. Furthermore, HR-TEM images revealed the crystalline nature of NPs and also showed that lattice fringes have a spacing of 0.235 nm for AgNPs and 0.239 nm for AuNPs, which reveals that the growth of these nanoparticles occurs preferentially on the (1 1 1) plane [29, 30]. HAADF images, elemental mapping, and EDX analysis confirmed that these are pure suspensions of Ag and Au nanoparticles, Fig. 3.

Results from ICP-OES and TEM measurements were then used to estimate the number of particles per milliliter. Approximately, 8.85×10^9 Au particles and 3.42×10^{11} Ag particles/ml were obtained by the PLAL method.

3.2 LIBS and NELIBS experiments

To determine the optimum experimental conditions a series of spatially resolved measurements were performed for Cr and Pb. Considering that the TISR method utilizes the fact that intense continuum emission is mostly emitted from a region close to the sample surface, the best signal-to-background (SBR) value was achieved by changing the viewing position of plasma along its expanding direction

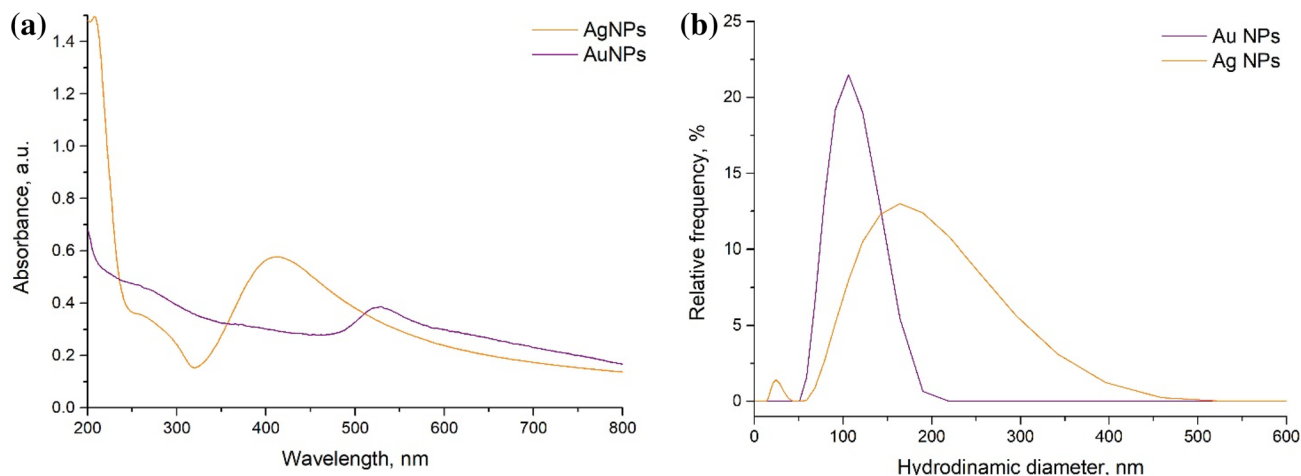


Fig. 1 **a** UV–Vis spectra of noble nanoparticles; absorbance for AuNPs is 3 times multiple for better clarity; **b** Hydrodynamic diameters of AuNPs and AgNPs measured by the DLS method

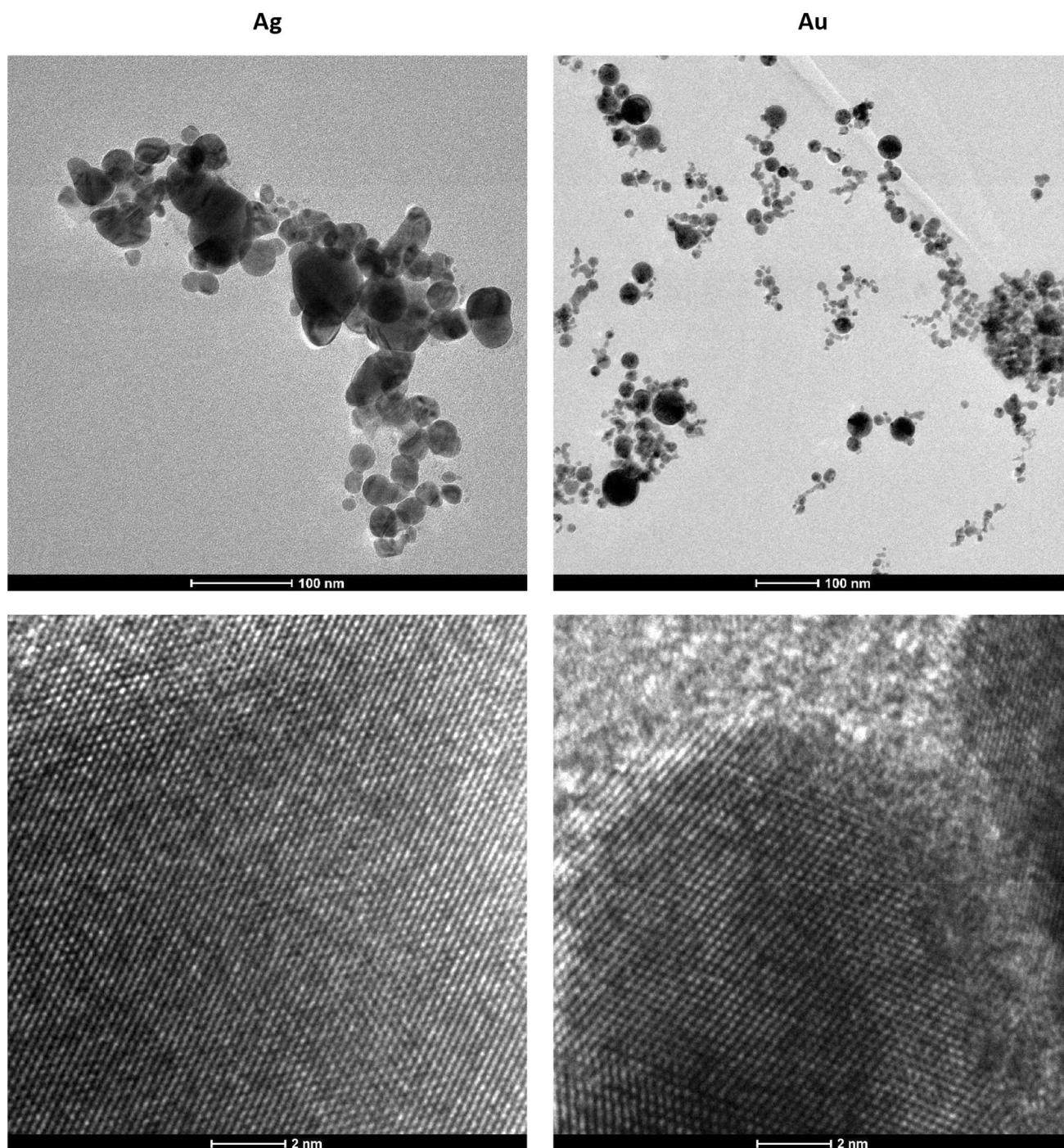


Fig. 2 TEM images of nanoparticles and lattice fringes of Ag and Au NPs

toward the laser beam [23]. After finding the plasma region with the best SBR value for these elements, TISR measurements were conducted. The surface area covered with NPs was approximately 3.2 mm^2 while the laser spot was approximately 1 mm^2 . Despite the fact that the laser-affected area is smaller than the covered area, obtained plasma was luminous and covered even beyond the

NPs-covered area. Furthermore, it has been noticed that a noticeable signal enhancement is only achieved when two laser shots per spot are applied. Since all measurements are time-integrated, each recorded spectrum represents an accumulation of consecutive spectra from 2 laser shots at one spot on three different sample areas. This procedure

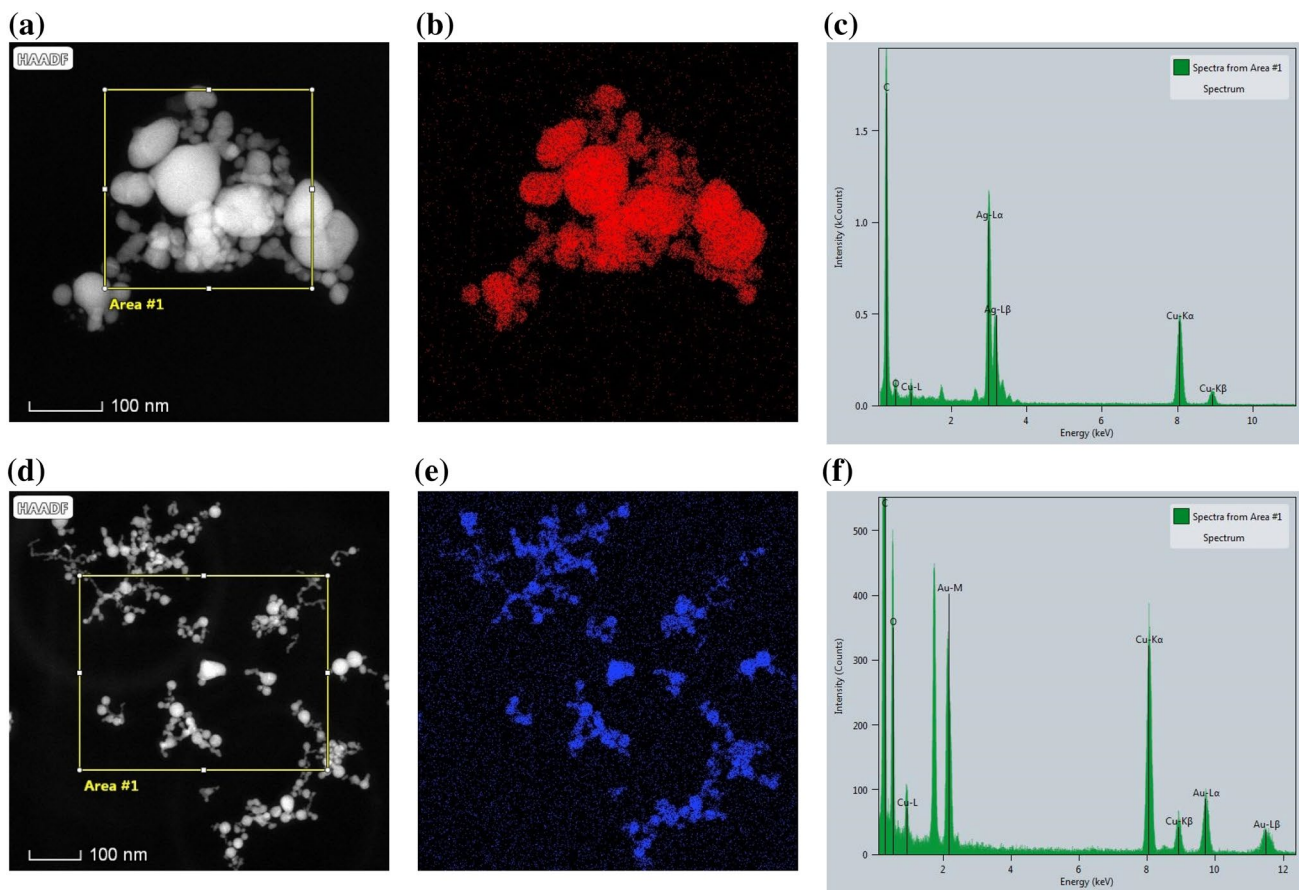


Fig. 3 HAADF-TEM images (a, d), elemental mapping (b, e) and EDX spectra (c, f) of Ag and Au nanoparticles

was replicated in triplicate and the resulting segments of averaged LIBS and NELIBS spectra are given in Fig. 4.

Sharp and well-resolved lines of Pb I 405.78 nm and Cr I 425.43 nm were used to estimate the effect of deposited nanoparticles on the measured signal. In addition, in obtained spectra several titanium lines were detected since titanium dioxide is one of the most widely used pigments in plastics, as it efficiently scatters visible and absorbs UV light, thereby imparting whiteness, brightness, and opacity [31]. These emission line profiles were reasonably well approximated by the Voigt line shape, and integrated peak areas were used for the estimation of the enhancement effects and limit of detection (LOD). The repeatability of the LIBS and NELIBS methods can be observed by the relative standard deviation of integrated areas. Obtained RSD values were similar in the case of LIBS and NELIBS with gold nanoparticles (around 30% for Cd, 18% for Pb), while in the case of AgNPs NELIBS RSD was 6% for Pb and 9% for Cd. Using the ratio between the area of an emission peak acquired with LIBS and the area of the same emission peak acquired by AuNPs and AgNPs NELIBS it was estimated that the enhancement of the Cd emission line was 14 and 45 times,

respectively. A similar trend was observed with Pb emission lines, and the enhancement was 26 and 52 times. Since there were no available standards in the time the experiment was conducted, LOD was calculated using the formula $LOD = (3 \times c) / SNR$, where c is a known analyte concentration obtained by the ICP-OES method (290 ± 20 mg/kg Cr, 1160 ± 50 mg/kg Pb in sample), and signal-to-noise ratio (SNR) is the absolute intensity of the integrated peak area A , divided by the width of the peak area w , times the absolute value of the rms noise, $SNR = A / (w \times rms)$ [32]. Obtained LOD results are summarized in Table 1.

3.3 Surface effects of noble nanoparticles

Characterization of the laser-affected areas of the sample surfaces was carried out using optical profilometry. Three-dimensional (3D) and linear profilometric analyses have been utilized to determine the effect of nanoparticles deposition on the resulting sample damages after the LIBS analysis. In Fig. 5, 3D and linear damage profiles of the sample surface before and after LIBS and NELIBS measurements are given. Further analysis showed that ablated volume was $1.9 \pm 0.4 \times 10^{15}$ nm³

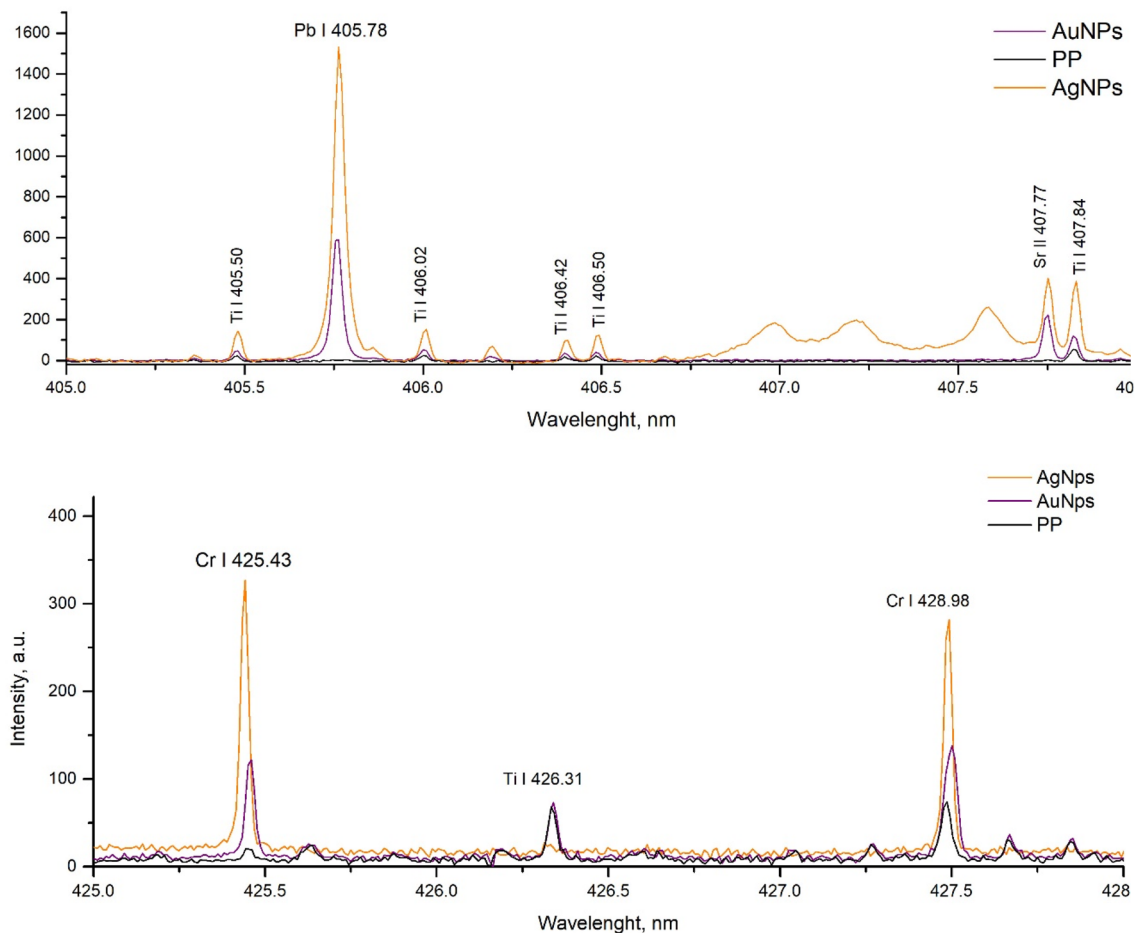


Fig. 4 Segments of LIBS and NELIBS spectra obtained by analyzing pure polypropylene sample (PP) or PP samples covered with AgNPs/AuNPs (AgNps, AuNps)

Table 1 Estimated limits of detection for Cr and Pb in plastic sample

Exp	LOD Cr, ppm	LOD Pb, ppm
LIBS	71.3	69.5
NELIBS Ag	4.4	4.1
NELIBS Au	10.9	5.4

in the case of classic LIBS measurements, while when Ag and Au nanoparticles were applied ablated volumes were higher, $5.4 \pm 0.8 \times 10^{15} \text{ nm}^3$ and $5.0 \pm 0.7 \times 10^{15} \text{ nm}^3$, respectively. Based on obtained results it can be concluded that the slightly higher sample volume was ablated during the NELIBS experiment.

4 Discussion

Based on the represented results, enhancement was achieved for both NPs. There are several differences. The difference between measured nanoparticle diameters by TEM and DLS methods is because the DLS obtained value presents the size of the nanoparticles in their hydrated state, together with the surrounding layers of water molecules that extend the hydrodynamic diameter and make the hydrated shell around the particle significantly larger than the particles themselves, or more likely, the diameter differences are arising because the NPs in colloidal solutions are subject to aggregation, as visible in the SPR spectra. For this reason, results obtained by TEM analysis were used to estimate the number of nanoparticles per milliliter in the colloid solution obtained by the PLAL method. Furthermore, the number of AgNPs is 38 times greater than the number of AuNPs in the solution. Nevertheless, the resulting difference in the enhancement of the emission signal is only 2–3 times greater in the favor of Ag. Based on the recent publication Dell'Anglio et al. the further optimization of the optimal

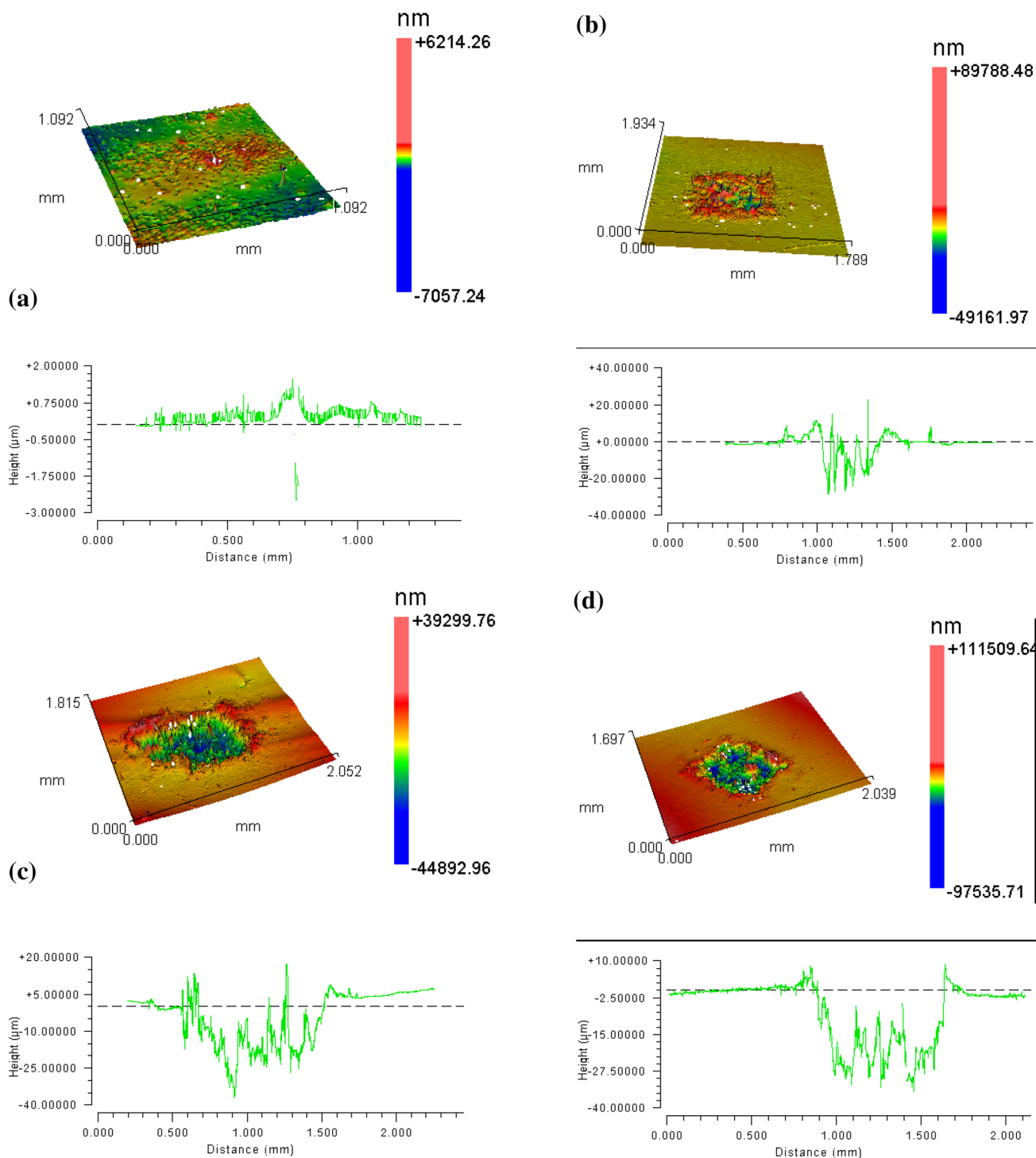


Fig. 5 3D and linear profilometric analyses of the polypropylene surfaces **a** before irradiation **b** after irradiation with TEA CO₂ laser without deposited nanoparticles, **c** after irradiation with TEA CO₂

laser, with deposited gold nanoparticles, and **d** after irradiation with TEA CO₂ laser, with deposited silver nanoparticles

number of NPs per unit surface should be performed to come to an accurate conclusion [15]. There is also a difference in the reflectivity of these two metals for the applied laser wavelength. Since to the best of our knowledge, there is no report

for the studies regarding the reflectivity of noble metal nanoparticles at 10.6 µm, the closest relevant study was performed by Bennet and Ashley [33]. They reported that ultra-high vacuum silver foil has a reflectance of 0.9953 while the gold

measured value is 0.9939 for 10 μm wavelength. In fact, silver has the highest infrared reflectance of any known material. On the other side, with the heating of nanoparticles to high temperatures, intensive thermal radiation can be expected. This phenomenon is explained very well in the investigation regarding the efficiency of losses in nanomaterials production technologies, for dimensions smaller than the wavelength at the maximum radiation spectrum in dependence on the temperature and conductivity of particles [34]. Furthermore, surface plasmon resonance of these nanoparticles can be achieved only at a specific wavelength in the visible part of the spectrum, meaning that underlying mechanisms responsible for NELIBS enhancement of signal in our experiments cannot be explained by the plasmonic effect. To our best knowledge, this is the first paper that confirms the possibility of using TEA CO_2 laser for NELIBS applications, considering that already mentioned Kiris et al. [16] are the only ones who have so far investigated the prospect of using this type of laser for NELIBS, had the lack of enhancement of analyte signal during use copper oxide nanoparticles deposited on polytetrafluoroethylene. The relative standard deviation of LIBS (24% for Cr, 18% for Pb) and NELIBS Integrated peak areas of Cr and Pb was calculated, and it was noticed that the RSD values decreased when AgNPs (9% for Cr, 5% for Pb) were used, while when AuNPs (40% for Cr, 16% for Pb) were employed, these values were similar to in the LIBS analysis. In the comparative study, Lui et al. showed that the repeatability of NELIBS was lower than that of LIBS except for silicon wafer, in which the reflection of laser light seemed to play an important role in making the difference [35]. These preliminary results can be related to the method of acquisition of emission spectra since they represent the accumulated spectra of 2 laser shots. Considering that the Maximum Concentration Value (MCV) for Pb and Cr covered by Restriction of Hazardous Substances (RoHS) is 0.1%, it can be assumed that the NELIBS method developed in this work be well suited as a fast and reliable screening method of Pb and Cr in plastic materials within the RoHS directive.

While TEA CO_2 -based NELIBS can produce lower LOD values, profilometric measurements showed that the amount of ablated material was greater than in the LIBS experiment. As the NELIBS is considered a good method for the elemental analysis of transparent samples such as gemstones or precious cultural relics [35], it cannot be considered a non-destructive method.

5 Conclusions

In this paper, we have proposed a variant of an unconventional LIBS based on TEA CO_2 laser on the use of silver and gold NPs, synthesized by the PLAL method, to enhance the emission intensity of plastic. The limit of detection for both elements is over 10 times lower than the limit of

detections without deposition of an NP's colloidal solution. Moreover, an increase in the amount of material ejected during NELIBS was observed by profilometric analysis. The NELIBS method developed in this work is well-suited as a fast and reliable screening method for Pb and Cr in plastic materials within the RoHS directive.

Acknowledgements Authors thank the Ministry of Science, Technological Development, and Innovation of the Republic of Serbia for the financial support to the research through institutional funding (Contract number 451-03-47/2023-01/200017); bilateral project between Serbia and Croatia (337-00-205/2019-09/15); Croatian Science Foundation under project HrZZ-IP-2019-04-6418)

Author contributions Conceptualization, MM and SŽ; methodology, SŽ; formal analysis, JP, MN, JC; investigation, NK, MO; data curation, SŽ; writing—original draft preparation, MM; writing—review and editing, SŽ; All authors have read and agreed to the published version of the manuscript.

Data availability The data that support the findings of this study are available from the corresponding author, upon reasonable request.

Declarations

Conflict of interest The authors declare no conflict of interest. The authors have no relevant financial or non-financial interests to disclose.

References

1. A. Turner, M. Filella, *Environ. Int.* **156**, 106622 (2021)
2. R.-K. Matti, V. Pasi, K. Jukka, S. Antti, R. Milena, *Ash forming elements in plastics and rubbers* (Publisher VTT Technical Research Centre of Finland, Espoo, 2014) pp. 131
3. Y. Wang, H. Su, Y. Gu, X. Song, J. Zhao, *Onco. Targets. Ther.* **10**, 4065 (2017)
4. A.L. Wani, A. Ara, J.A. Usmani, *Interdiscip. Toxicol.* **8**, 55 (2015)
5. K. Liu, D. Tian, C. Li, Y. Li, G. Yang, Y. Ding, *TrAC. Trends Anal. Chem.* **110**, 327 (2019)
6. D.W. Hahn, N. Omenetto, *Appl. Spectrosc.* **66**, 347 (2012)
7. L. Jolivet, M. Leprince, S. Moncayo, L. Sorbier, C.-P. Lienemann, V. Motto-Ros, *Spectrochim. Acta Part B At. Spectrosc.* **151**, 41 (2019)
8. A. De Giacomo, R. Gaudiuso, C. Koral, M. Dell'Aglio, O. De Pascale, *Spectrochim. Acta Part B At. Spectrosc.* **98**, 19 (2014)
9. M. Dell'Aglio, R. Alrifai, A. De Giacomo, *Spectrochim. Acta Part B At. Spectrosc.* **148**, 105 (2018)
10. M. Abdelhamid, Y.A. Attia, M. Abdel-Harith, *J. Anal. At. Spectrom.* **35**, 2982 (2020)
11. V.V. Kiris, A.V. Butsen, E.A. Ershov-Pavlov, M.I. Nedelko, A.A. Nevar, *Int. J. Nanosci.* **18**, 1940022 (2019)
12. D.J. Palásti, P. Albrycht, P. Janovszky, K. Paszkowska, Z. Geretovszky, G. Galbács, *Spectrochim. Acta Part B At. Spectrosc.* **166**, 105793 (2020)
13. Z. Salajková, V. Gardette, J. Kaiser, M. Dell'Aglio, A. De Giacomo, *Spectrochim. Acta Part B At. Spectrosc.* **179**, 106105 (2021)
14. X. Liu, Q. Lin, Y. Tian, W. Liao, T. Yang, C. Qian, T. Zhang, Y. Duan, *J. Anal. At. Spectrom.* **35**, 188 (2020)
15. M. Dell'Aglio, C. Di Franco, A. De Giacomo, *J. Anal. At. Spectrom.* (2023). <https://doi.org/10.1039/D2JA00324D>. <https://pubs.rsc.org/en/content/articlelanding/2023/JA/D2JA00324D>

16. V. Kiris, J. Savovic, A. Nevar, M. Kuzmanovic, M. Nedelko, D. Rankovic, N. Tarasenko, *Spectrochim. Acta Part B At. Spectrosc.* **187**, 106333 (2022)
17. G.K. Yogesh, S. Shukla, D. Sastikumar, P. Koinkar, *Appl. Phys. A* **127**, 810 (2021)
18. N. Krstulović, K. Salamon, O. Budimlija, J. Kovač, J. Dasović, P. Umek, I. Capan, *Appl. Surf. Sci.* **440**, 916 (2018)
19. Y. Jing, R. Wang, Q. Wang, Z. Xiang, Z. Li, H. Gu, X. Wang, *Adv. Compos. Hybrid Mater.* **4**, 885 (2021)
20. D. Blažeka, R. Radičić, D. Maletić, S. Živković, M. Momčilović, N. Krstulović, *Nanomaterials* **12**, 2677 (2022)
21. M. Momcilovic, M. Kuzmanovic, D. Rankovic, J. Ciganovic, M. Stoiljkovic, J. Savovic, M. Trtica, *Appl. Spectrosc.* **69**, 419 (2015)
22. J. Savovic, M. Stoiljkovic, M. Kuzmanovic, M. Momcilovic, J. Ciganovic, D. Rankovic, S. Zivkovic, M. Trtica, *Spectrochim. Acta Part B At. Spectrosc.* **118**, 127 (2016)
23. J.J. Savović, S.M. Živković, M. Momčilović, M. Trtica, M. Stoiljković, M. Kuzmanović, *J. Serbian Chem. Soc.* **82**, 1135 (2017)
24. S. Zivkovic, J. Savovic, M. Trtica, J. Mutic, M. Momcilovic, *J. Alloys Compd.* **700**, 175 (2017)
25. S. Zivkovic, M. Momcilovic, A. Staicu, J. Mutic, M. Trtica, J. Savovic, *Spectrochim. Acta Part B At. Spectrosc.* **128**, 22 (2017)
26. S. Zivkovic, J. Savovic, M. Kuzmanovic, J. Petrovic, M. Momcilovic, *Microchem. J.* **137**, 410 (2018)
27. M. Weidman, M. Baudelet, S. Palanco, M. Sigman, P.J. Dagdigan, M. Richardson, *Opt. Express* **18**, 259 (2010)
28. J. Car, D. Blažeka, T. Bajan, L. Krce, I. Aviani, N. Krstulović, *Appl. Phys. A* **127**, 838 (2021)
29. M.A. Majeed Khan, S. Kumar, M. Ahamed, S.A. Alrokayan, M.S. AlSalhi, *Nanoscale Res. Lett.* **6**, 434 (2011)
30. L. Wang, W. Zhang, D. Sheng Su, X. Meng, F.-S. Xiao, *Chem. Commun.* **48**, 5476 (2012)
31. L.W. McKeen, in *Permeability Prop. Plast., Elastomers* (William Andrew, Norwich, NY, 2017), pp. 21–40
32. B.T. Fisher, H.A. Johnsen, S.G. Buckley, D.W. Hahn, *Appl. Spectrosc.* **55**, 1312 (2001)
33. J.M. Bennett, E.J. Ashley, *Appl. Opt.* **4**, 221 (1965)
34. Y.V. Martynenko, L.I. Ognev, *Tech. Phys.* **50**, 1522 (2005)
35. J. Liu, Z. Hou, T. Li, Y. Fu, Z. Wang, *J. Anal. At. Spectrom.* **35**, 2274 (2020)

Publisher's Note Springer Nature remains neutral with regard to jurisdictional claims in published maps and institutional affiliations.

Springer Nature or its licensor (e.g. a society or other partner) holds exclusive rights to this article under a publishing agreement with the author(s) or other rightsholder(s); author self-archiving of the accepted manuscript version of this article is solely governed by the terms of such publishing agreement and applicable law.